

## 1. Introduction



Figure 1: Suspension coil spring. Coil diameter D and wire diameter d are shown.

Nowadays lightweight automotive construction is one of the innovative forces in the automotive industry. Climate change objectives, urbanization, scarcity of raw materials, new vehicle concepts and legal regulations for CO<sub>2</sub> emission are driving the efforts of car manufacturers towards lightweight construction. This applies in particular to the components of the unsprung mass of a vehicle, e.g. for vehicle suspension springs made from spring steel.

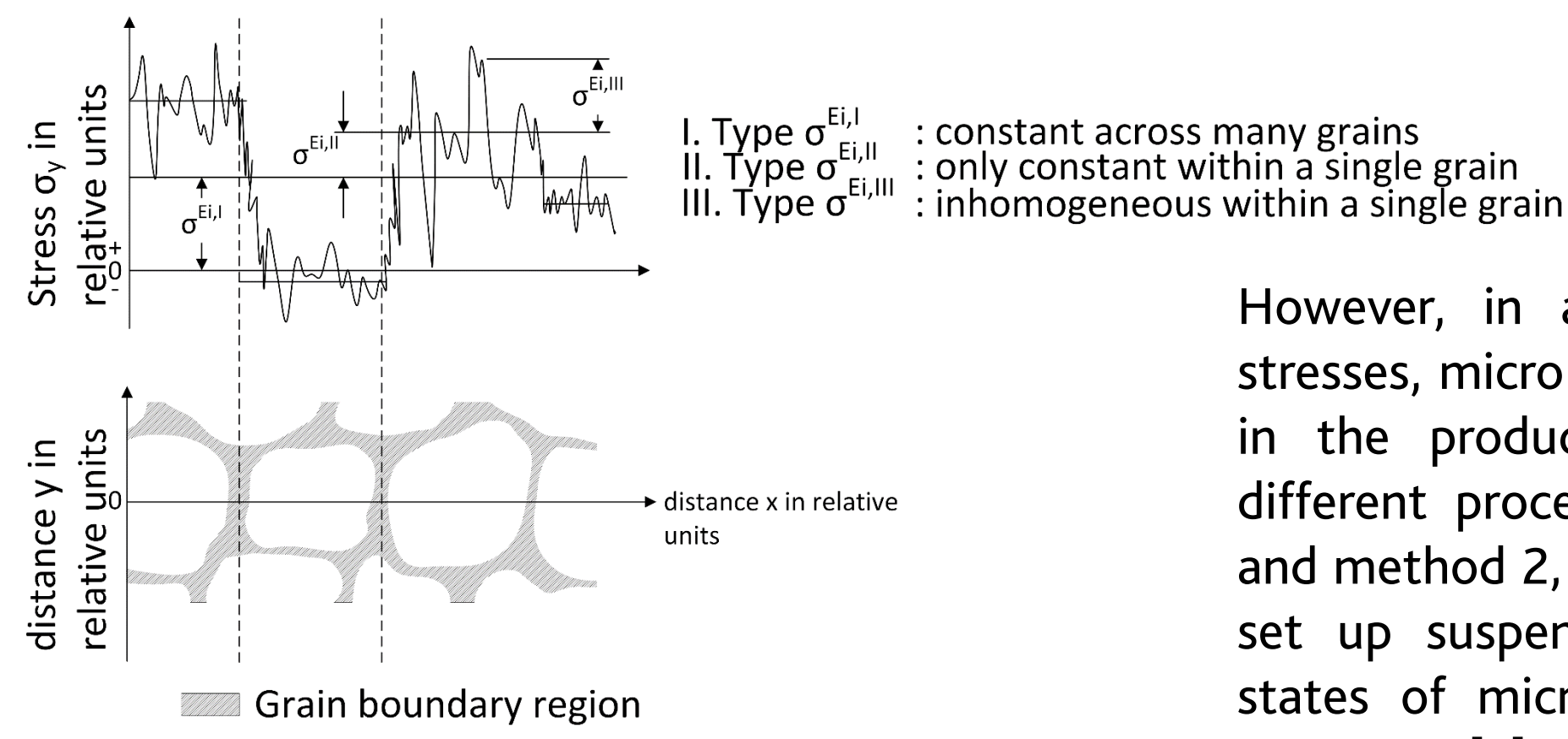


Figure 2: Definition of the macro and micro residual stresses according to Macherauch [1]

However, in addition to the macro residual stresses, micro residual stresses are also built up in the production processes. Therefore, two different process routes denoted as method 1 and method 2, respectively, have been chosen to set up suspension coil springs with different states of micro residual stresses. A study by Bauschke [2] shows up that the magnitude of micro residual stresses has a certain impact on the fatigue life of suspension coil springs. This is shown in Figure 3.

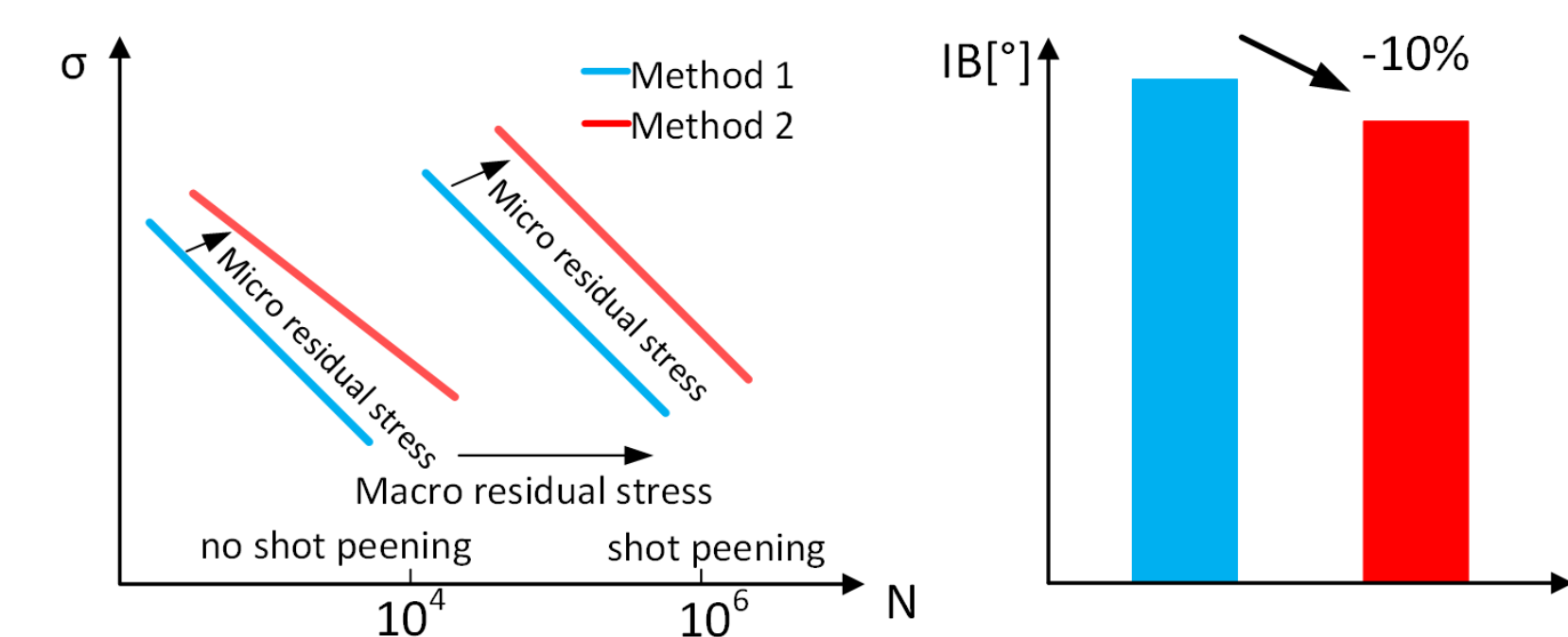


Figure 3: The impact of macro & micro residual stresses on the fatigue life of coil springs [2]

## 2. Stress Analysis

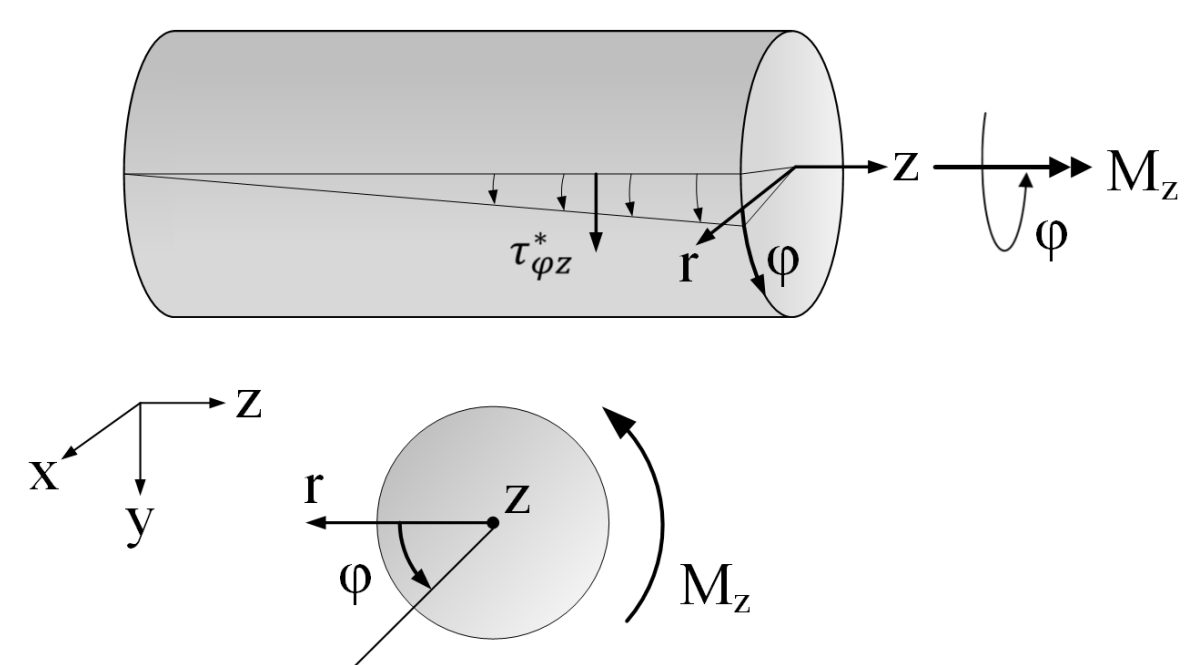


Figure 4: Stress distribution of a torsion bar

The stress distribution of a coil spring under load is reasonably well described by a model of the torsion bar (s. Figure 4). The principal stresses are given by

$$\bar{\sigma}_{\tau,H}^*(r) = \begin{pmatrix} 0 & 0 & 0 \\ 0 & \tau_{\varphi z}^*(r) & 0 \\ 0 & 0 & -\tau_{\varphi z}^*(r) \end{pmatrix}$$

where

$$\tau_{\varphi z}^*(r) = \frac{2M_z}{\pi r_{max}^4} r$$

A setting process leads to a plastic deformation with a resultant residual stress profile which is given according to Kobelev [3] by

$$\sigma^{Ei,S}(x) = \begin{cases} \tau_0 - \Delta\theta \cdot G \left(1 - \frac{x}{r_{max}}\right), & r \geq r_{pl} \\ \theta_{res} \cdot G \left(1 - \frac{x}{r_{max}}\right), & r < r_{pl} \end{cases}$$

which denotes the principal stress component #2. The remaining symbols are:

- $\tau_0$ : Shear stress at the surface
- $\Delta\theta$ : Elastic spring back
- $\theta_{res}$ : Residual plastic deformation

Huge compressive residual stresses in the surface area are established during a shot peening processes. According to [4] this residual stress profile is given here by

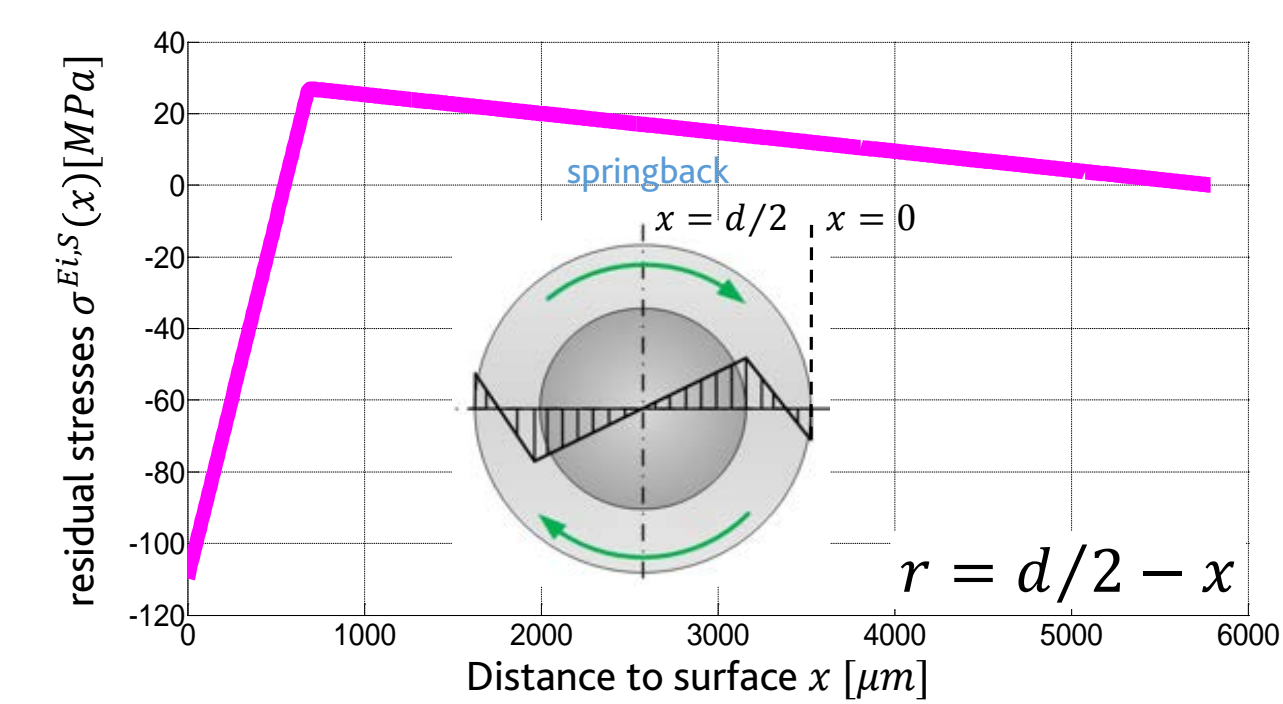


Figure 5: Residual stress profile of a torsion bar after a setting procedure

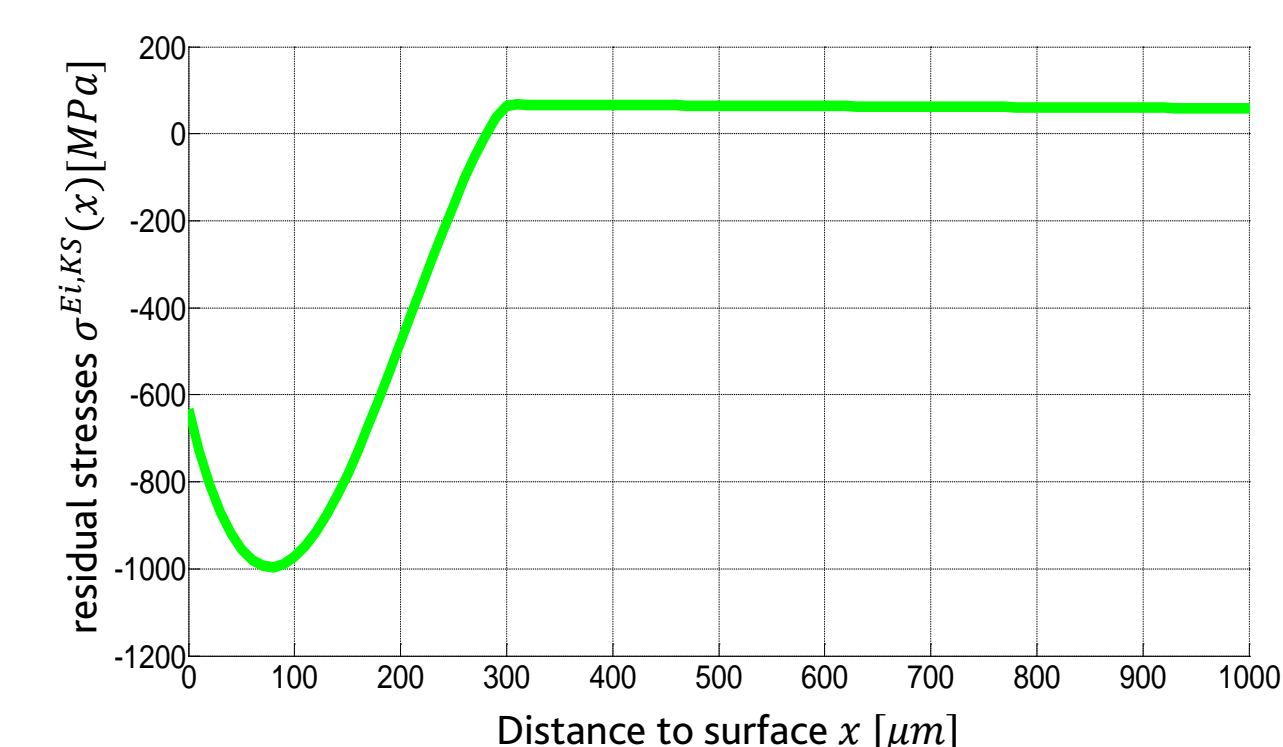


Figure 6: Residual stress profile of a torsion bar after a shot peening procedure

$$\sigma^{Ei,KS}(x) = \begin{cases} -0.0001 \cdot x^3 + 0.08 \cdot x^2 - 10.115 \cdot x - 633.6 & \text{for } 0 \ll x \leq x_2 \\ 67.074 \cdot \sin(0.1(x - 281)) & \text{for } x_2 \ll x \leq x_s \\ -0.012 \cdot (x - 304) + 67.1 & \text{for } x_s \ll x \leq d/2 \end{cases}$$

The stress distribution of a coil spring under load considering the residual stresses by setting and shot peening is approximately given by

$$\bar{\sigma}_H = \begin{pmatrix} 0 & 0 & 0 \\ 0 & \sigma_2 & 0 \\ 0 & 0 & \sigma_3 \end{pmatrix} = \begin{pmatrix} 0 & 0 & 0 \\ 0 & \tau_{\varphi z}^*(r) + \sigma^{Ei,S}(r) + \sigma^{Ei,KS}(r) & 0 \\ 0 & 0 & -\tau_{\varphi z}^*(r) - \sigma^{Ei,S}(r) + \sigma^{Ei,KS}(r) \end{pmatrix}$$

## 3. Modelling of Fatigue Strength

Kletzin et al. [5] recently investigated the fatigue strength of coil springs. They developed the following scheme based on the FKM guideline [6] showing the transition from a material property, i.e. the tensile strength  $R_{mV}$  to the finite life fatigue strength of the component.

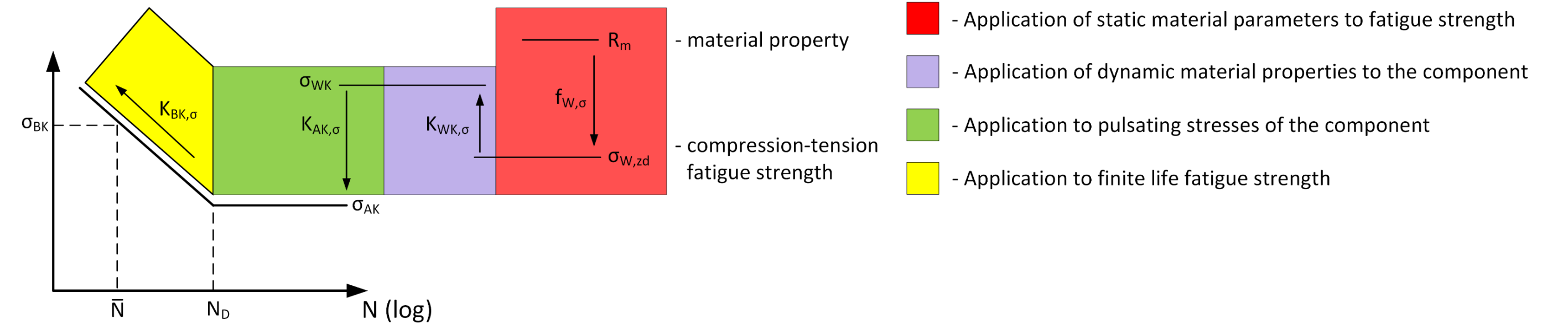


Figure 7: Fatigue strength assessment according to the FKM guideline [5]

A concept of local fatigue strength is described by Kletzin et al. [5] as well which is based on the fundamental approach of Macherauch [7]. This concept is the basis of this model and it will be further developed in this work.

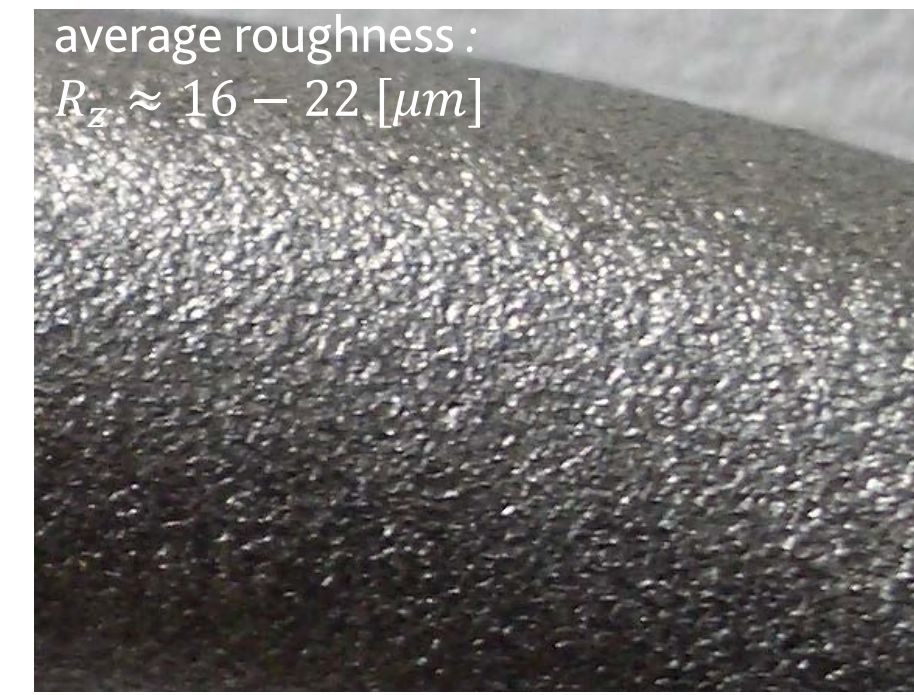


Figure 8: Surface of a coil spring wire after shot peening [9]

Here the principal stresses are considered. Hence, the tension - compression fatigue strength  $\sigma_{W,z,d}$  of the material can be transformed to become the component fatigue strength  $\sigma_{WK,\sigma}$  by using the design factor  $K_{WK,\sigma}$ . This factor includes in this model the surface roughness factor and a stress correction factor  $k$  by Bergsträsser [8] for coil springs.

The local fatigue strength of a coil spring at the surface and below the surface is given by

$$\begin{aligned} \sigma_{AK,\sigma} &= 0.75 \cdot \sigma_{WK} - 0.2 \cdot \tau_{\varphi z,m}^* - M_1 \cdot \sigma^{Ei,S} - M_2 \cdot \sigma^{Ei,KS} & \text{at the surface} \\ \sigma_{AK,\sigma} &= 0.75 \cdot \sigma_{W,z,d} - 0.2 \cdot \tau_{\varphi z,m}^* - M_1 \cdot \sigma^{Ei,S} - M_2 \cdot \sigma^{Ei,KS} & \text{below the surface} \end{aligned}$$

where  $\tau_{\varphi z,m}^*$  is the mean stress and  $M_1 = M_2 = 0.2$  denote the residual stress sensitivity factors.

## 4. Result

A local fatigue strength assessment has been conducted for 2 different types of springs, i.e. a suspension coil spring and a valve spring. The results are shown in the diagrams.

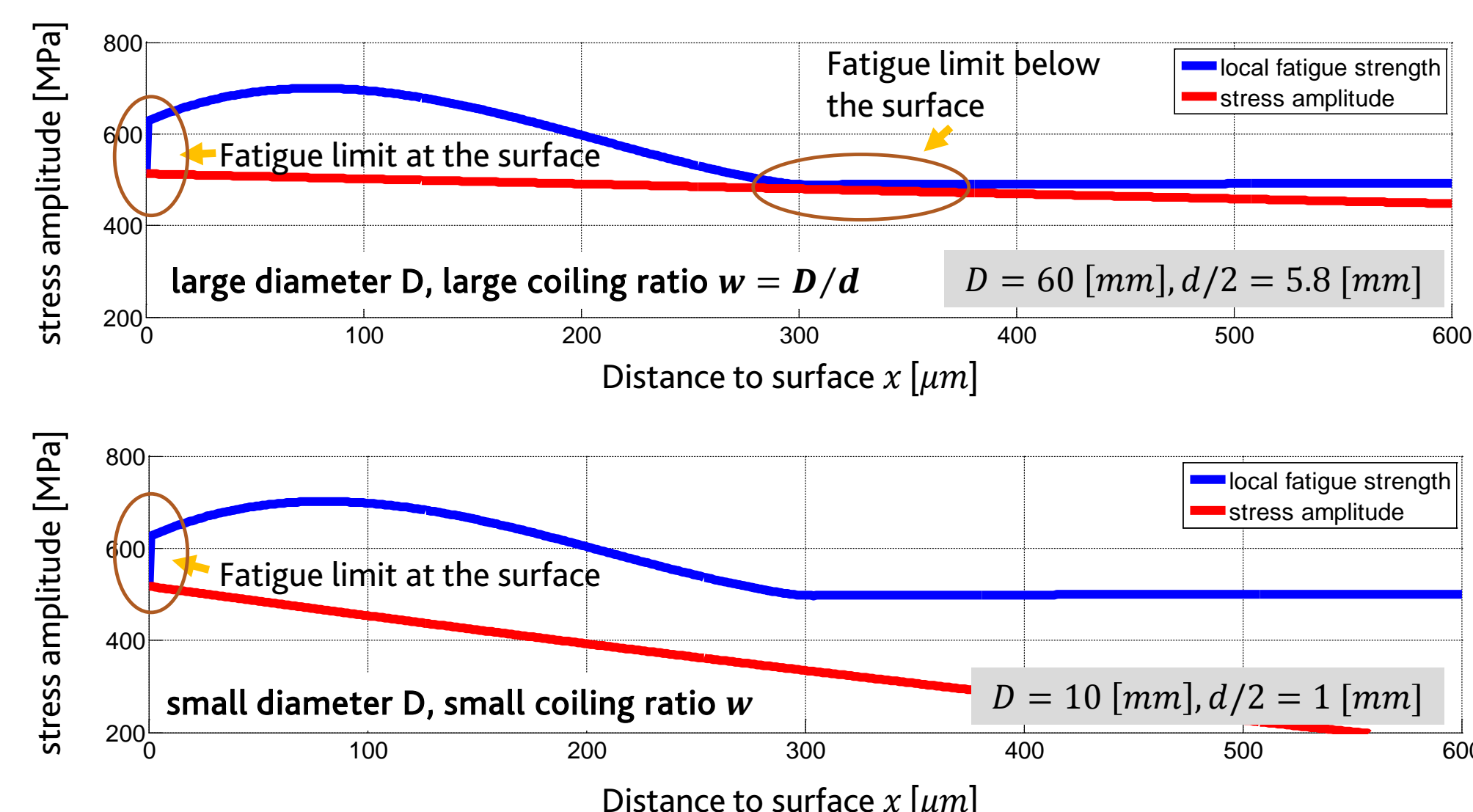


Figure 9: The local fatigue strength vs. the stress amplitude of a suspension coil spring and a valve spring.

The local fatigue strength of a coil spring, which is given by a blue line, shows a non homogeneous profile along the wire cross section. Starting from the surface it increases due to the residual stresses of the shot peening process. After a distance of 100  $\mu\text{m}$  it drops and it finally stays almost constant. The stress amplitude during fatigue testing, which is indicated by a red line, is decreasing with increasing distance from the surface.

The effect of size is clearly seen in the diagrams. The above diagram, which represents a suspension coil spring, shows that the stress amplitude reaches the local fatigue strength at the surface and below the surface as well.

## 5. Discussion and Outlook

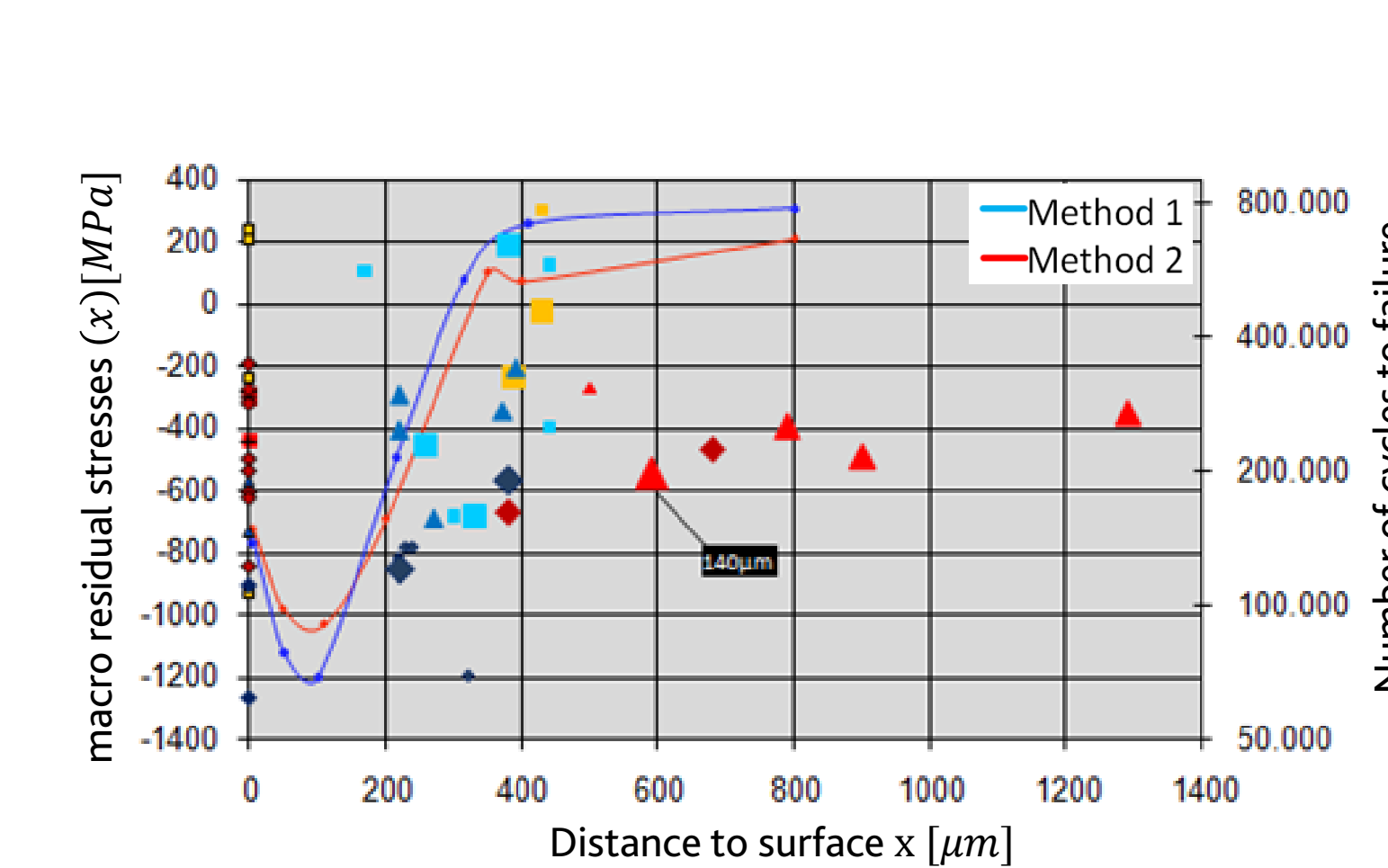


Figure 10: Location of fractures and the fatigue life of coil springs [2].

The results of fatigue testing by [2] show fractures starting from the surface and from sites below the surface. It is clearly seen, that no fractures starts in a distance of 20 - 180  $\mu\text{m}$  to the surface due to the apparent huge compressive residual stresses. However, springs made by method 1 more frequently start to fail in the region between 200 and 400  $\mu\text{m}$ . It is assumed here that this accumulation is closely related to the higher micro residual stresses compared to those springs made by method 2.

## 6. Literature

- [1] Macherauch, E. Neuere Untersuchungen zur Ausbildung und Auswirkung von Eigenspannungen in metallischen Werkstoffen, 1979
- [2] Bauschke, T., Weiß, H., Kobelev, V. Entstehung der Windeigenspannungen und deren Einfluss auf die Ermüdungslebensdauer bei kalt- und halbwarm geformten Fahrzeugfedern, Universität Siegen, 2011
- [3] Kobelev, V. Mechanik und Gestaltung von Stahlfedern. Attendorn: Mubea KG, 2012.
- [4] Hesse, C. Untersuchung des Eigenspannungseinflusses auf den Lastspannungszustand von Achsfedern zur Ermittlung eines möglichen Leichtbaupotentials, Universität Siegen, 2011
- [5] Kletzin, Lebensdaueruntersuchung für Schraubendruckfedern, Technische Universität Ilmenau
- [6] Rechnerischer Festigkeitsnachweis für Maschinenbauteile aus Stahl, Eisenguss- und Aluminiumwerkstoffen 4, erweiterte Ausgabe, 2002
- [7] Macherauch, E., Wohlfahrt, H. Ermüdungsverhalten metallischer Werkstoffe, Deutsche Gesellschaft für Materialkunde e.V., Oberursel, 1985
- [8] Warm geformte Federn, Konstruktion und Fertigung, Hoesch Hohenlimburg AG, 1987
- [9] Mubea Fahrwerksfedern GmbH, Attendorn, Germany